ISSN 1063-7737, Astronomy Letters, 2026, Vol. 52, No. 3, pp. 101–106. © Pleiades Publishing, Ltd., 2026.

Slowdown of Positrons Produced when Hard Background Gamma-Ray Photons Interact with Soft Background Photons

A. N. Popov[1], D. P. Barsukov[1*], A. V. Ivanchik[1], and S. V. Bobabshev[†1]

[1] *Ioffe Institute, Russian Academy of Sciences, St. Petersburg, 194021 Russia*

Received March 27, 2026; revised April 26, 2026; accepted May 13, 2026

Abstract—We consider the interaction of hard background gamma-ray photons with energies above 100 MeV with optical and X-ray background photons to produce electron–positron pairs by taking into account the accumulation of produced positrons and the subsequent energy loss by them when interacting with the cosmic microwave background. We show that a slow component of positrons with an energy below 1 MeV arises in this case, but the total number of slow positrons is only $\sim 0.01-0.1\%$ of the total number of positrons produced in this interaction.

DOI: 10.1134/S1063773726700271

Keywords: *slowdown of positrons, gamma-ray photons*

INTRODUCTION

The density of matter is measured in 1 g cm^{-3} in planets and the centers of stars and even in 10^{15} g cm^{-3} in the interiors of neutron stars, while the overwhelming volume of space between galaxies is filled with a highly rarefied gas whose number density reaches $\sim 10^{-3}$ cm^{-3} only in the centers of galaxy clusters (Vikhlinin et al. 2006). Nevertheless, a major contribution to the scattering of gamma-ray photons from distant sources going through the space between galaxies is made by their scattering precisely by this gas (Grebenev and Sunyaev 2020). However, besides, high-energy gamma-ray photons can interact with much more numerous background photons, with the production of electron–positron pairs when two photons collide being also possible for them in addition to their scattering (Gould and Schreder 1967). As a result, positrons can be produced in the space between galaxy clusters. Of course, hard background photons are also involved in this process. As a result, an additional source of positrons appears in the space between galaxy clusters. In contrast to galactic jets (Nizamov and Pshirkov 2023) and pulsars (Istomin et al. 2020), whose positrons are fairly localized near the galaxies or jet remnants, this source creates a spatially more or less homogeneous component of positrons. The production of such positrons was considered in detail previously by Popov et al. (2023a). In this paper, following Popov et al. (2023a, 2025), we consider how the positrons produced when hard, with energies $\varepsilon_\gamma > 100$ MeV, cosmic gamma-ray background (CGB) photons interact with soft optical extragalactic background light (EBL) and cosmic X-ray background (CXB) photons will lose their energy or, in other words, will slow down when scattered by cosmic microwave background (CMB) photons. We also provide an upper limit on the possible spectrum of positrons produced when CGB photons interact with hypothetical cosmic ultraviolet background (CUB) photons unless, of course, for some reason the spectrum of CUB photons is extremely small.

THE MODEL

In this paper we use the standard cosmological ΛCDM model (Ade et al. 2016). In this model the density of matter in the Universe can be described only by the contributions of dark energy and cold dusty dark matter assuming that the contribution of radiation and relativistic particles may be neglected, which is admissible at $z \ll z_{\rm eq} \approx 3365$ (Ade et al. 2016), where z is the redshift and $z_{\rm eq}$ is the redshift corresponding to hydrogen recombination. In this case, the z dependence of the Hubble parameter can be described as

$$H(z) = H_0\,(1+z)\,\sqrt{\Omega_\Lambda + \Omega_M\,(1+z)^3}, \quad (1)$$

where the constants $\Omega_\Lambda \approx 0.691$ and $\Omega_M \approx 0.309$ describe the contributions of dark energy and dark matter, respectively, and $H_0 \approx 67.7$ km s^{-1} Mpc^{-1} is the Hubble constant at $z = 0$ (Ade et al. 2016).

[†] Deceased.

[*] E-mail: bars.astro@mail.ioffe.ru

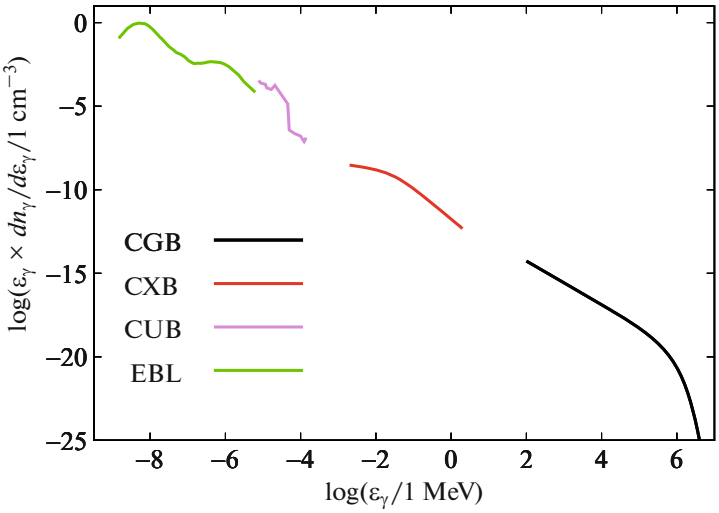


Fig. 1. The spectrum of background photons for $z = 0$ being used. The photon energy ε_γ is measured in 1 MeV; the photon number density $dn_\gamma/d\varepsilon_\gamma$ is measured in в 1 $\mathrm{cm}^{-3}\mathrm{MeV}^1$.

The model from Ackermann et al. (2015) is used to find the CGB spectrum. According to this model, the spectrum of its sources is assumed to be (Ackermann et al. 2015) $dq/d\varepsilon_\gamma = N_0\, S(z)\, \varepsilon^{-\gamma}\, \theta(\varepsilon_\gamma - \varepsilon_\gamma^{\max})$, where $dq/d\varepsilon_\gamma$ is the number of gamma-ray photons that are produced in 1 s in 1 cm^3 and have an energy ε_γ lying in a unit interval $d\varepsilon_\gamma$, $S(z)$ is the mean star formation rate in the Universe, and $\theta(x)$ is the Heaviside function (Ackermann et al. 2015). All quantities are given in the comoving frame. In this paper we assumed that $\gamma = 2.3$ and $\varepsilon_\gamma^{\max} = 3$ TeV (Ackermann et al. 2015). The parameter N_0 was chosen so that the resulting CGB photon flux at $\varepsilon_\gamma = 20$ GeV for $z = 0$ coincided with the observed value. As the function $S(z)$ we used its approximation from Behroozi et al. (2013):

$$S(z) = \frac{C}{10^{A\,(z-z_0)} + 10^{B\,(z-z_0)}}, \qquad (2)$$

where $z_0 = 1.243$, $A = -0.997$, $B = 0.248$, and $C = 0.180\ M_\odot\ \mathrm{yr}^{-1}\ \mathrm{Mpc}^{-1}$ (Behroozi et al. 2013). We considered only $z \le 3$ and assumed that the contribution of CGB photons produced at redshifts $z > 3$ was neglected. For simplicity, in this paper the spectra of CXB, CUB, and EBL photons were assumed to be independent of z and proportional to the star formation rate $S(z)$, i.e., the spectrum of soft background photons was assumed to be $dn_\gamma/d\varepsilon_\gamma = dn_\gamma/d\varepsilon_\gamma|_{z=0} \cdot (S(z)/S(0))$. The spectra of EBL and CXB photons for $z = 0$ were taken from Franceschini et al. (2008) and Ajello et al. (2008), respectively; as the spectrum of CUB photons we used the upper limits for their spectrum from Hill et al. (2018). The spectrum of background photons for $z = 0$ being used, i.e., $dn_\gamma/d\varepsilon_\gamma|_{z=0}$, is shown in Fig. 1. As shown in Popov et al. (2023a), the spectrum of produced positrons does not depend very strongly on what dependence of the number density of soft background photons on the redshift z we use in this model. Therefore, in this paper we restricted ourselves to the simplest extreme case where the spectrum of soft background photons is instantaneously adjusted to the number of their sources, which, for simplicity and uniformity, we took to be proportional to the star formation rate $S(z)$, no matter what the nature of these sources is (see, e.g., Hill et al. 2018; Cooray 2016; Franceschini et al. 2008). The dependence of the number density of CGB photon sources on the redshift z exerts a much stronger influence on the spectrum of produced positrons (Popov et al. 2023a; see also Ackermann et al. 2015). It also depends strongly on the choice of the spectrum of produced CGB photons. In this paper, as in Popov et al. (2023a, 2025), we took the parameter γ to be $\gamma = 2.3$, since we obtained the spectrum of CGB photons at $z = 0$ that resembles most closely the observed spectrum of CGB photons precisely for this value. The dependence of the spectrum of CGB photons in the model under consideration on the behavior of the number density of sources and their spectrum was studied in detail by Ackermann et al. (2015). The cross section for the interaction of soft background photons with CGB photons to produce electron–positron pairs was taken from Gould and Schreder (1967). The resulting production rate of electron–positron pairs was studied in detail by Popov et al. (2023a, 2023b). In this paper, as in Popov et al. (2025), we assumed that the produced positrons subsequently interact only with CMB photons. Since the produced

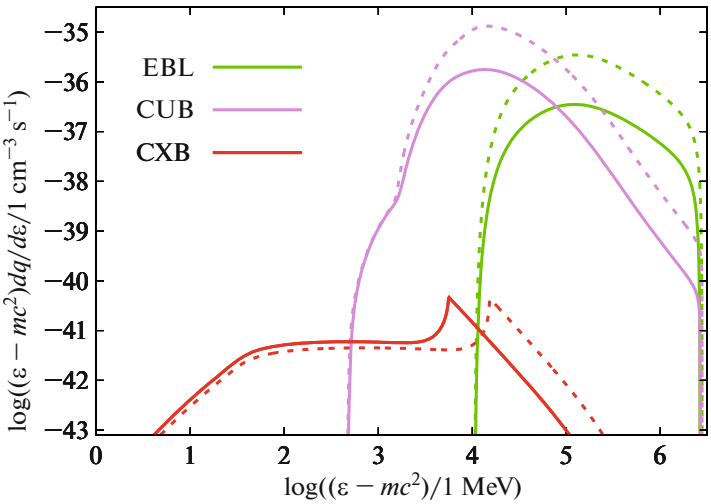


Fig. 2. The spectrum of produced positrons is indicated by the solid line for $z = 0$ and the dashed line for $z = 2$. The positron energy ε is measured in 1 MeV; the positron production rate $dq/d\varepsilon$ is measured in 1 cm^{-3} $\mathrm{s}^{-1}\mathrm{MeV}^1$ in the comoving frame.

positrons have an energy ε no more than $\varepsilon_\gamma^{\max}$ and we consider low $z \lesssim 3$, when the CMB temperature is low, $T_{\mathrm{CMB}} \lesssim 15$ K, in the positron rest frame the energy on the incoming photons is $\varepsilon_\gamma \ll mc^2$, where m is the positron rest mass, and, consequently, the cross section for the scattering of CMB photons by positrons may be considered in the Thomson limit. Accordingly, the energy of the scattered photon ε_γ^s is low compared to the positron energy ε, and this scattering may be considered as a continuous force of friction $\mathcal{P}$ that leads to the energy losses of positrons, i.e., slows them down, where

$$\mathcal{P} = \frac{4}{3}\,\mathrm{c}\,\sigma_{\mathrm{T}}\left(\frac{\varepsilon}{mc^2}\right)^2 \epsilon_{\mathrm{CMB}}. \qquad (3)$$

Here, $\mathcal{P}$ is the amount of energy being lost by the positron in 1 s, ε is its energy, ϵ_{CMB} is the CMB energy density, and σ_{T} is the Thomson scattering cross section. All quantities are measured in the comoving frame. The positron energy (ε) distribution function can then be found (at $\varepsilon \gg mc^2$) from the equation (Popov et al. 2025)

$$\frac{\partial}{\partial t}\left(\frac{dn}{d\varepsilon}\right) + 2\frac{H(z)}{1+z}\frac{dn}{d\varepsilon} - \frac{H(z)}{1+z}\varepsilon\frac{\partial}{\partial\varepsilon}\left(\frac{dn}{d\varepsilon}\right) = \frac{\partial}{\partial\varepsilon}\left(\mathcal{P}\left(\frac{dn}{d\varepsilon}\right)\right) + \frac{dq}{d\varepsilon}, \qquad (4)$$

where $dn/d\varepsilon$ is the number density of positrons with energies ε lying in the interval $d\varepsilon$ and t is the time. All quantities are measured in the comoving frame. The second and third terms on the left-hand side of the equation describe the change in the number density of positrons as the Universe expands and the influence of the redshift on their spectrum.

RESULTS

Figure 2 shows $dq/d\varepsilon$, i.e., the spectrum of positrons produced when background photons interact, for the redshifts $z = 0$ and 2. The spectrum of accumulated positrons that have already lost some of their energy due to the interaction with the CMB is shown in Figs. 3–5 for $z = 0$, 1, and 2, respectively. It can be seen that although the positrons produced when hard CGB photons interact with EBL photons and with the "upper limit" of hypothetical CUB photons have energies $\varepsilon \sim 1\,\mathrm{GeV}{-}1\,\mathrm{TeV}$, already at $z = 2$ the bulk of the positrons have energies $\varepsilon \sim 10{-}10^2$ MeV and a fairly noticeable slow component of positrons with energies $\varepsilon \lesssim 1$ MeV appears by $z = 1$, while by the present time $z = 0$ the bulk of the positrons still have energies $\varepsilon \sim 10{-}10^2$ MeV, with the slow component already beginning to account for $\sim 10^{-4}{-}10^{-3}$ of the total number of positrons produced in the process under consideration. Thus, it follows from Figs. 3–5 that the positrons lose their energy very efficiently when interacting with the CMB up to energies $\varepsilon \sim 10{-}10^2$ MeV, with the further decrease in their energy being much slower, which is an elementary consequence of the formula for the rate of energy loss by the positrons $\mathcal{P} \sim \varepsilon^2$ being used. As regards the positrons produced during the interaction of CGB and CXB photons, although their initial energy is noticeably lower, in view of the latter the energy losses for them due to the interaction with the CMB are also smaller. Moreover, since the CXB photons are generally few in number compared to the EBL photons, their contribution both to the total number of positrons and to the slow component is less than 10^{-3} and, accordingly, they may be calmly neglected. Formally, the upper limit on the

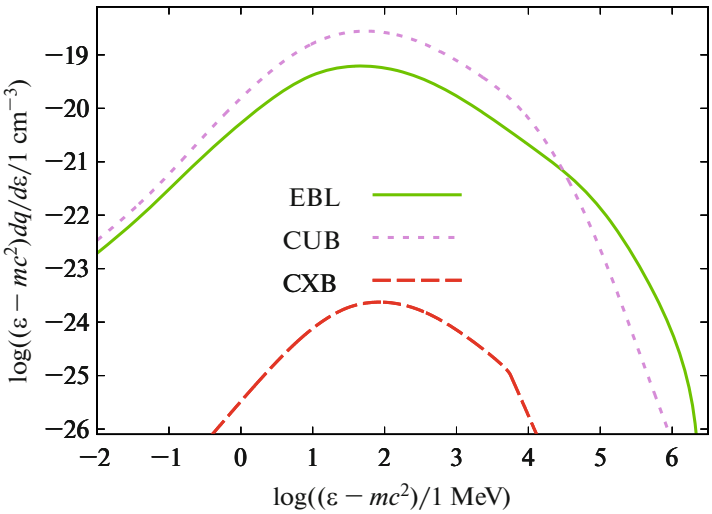


Fig. 3. The spectrum of positrons for $z = 0$ including their energy losses due to the interaction with the CMB. The positron energy ε is measured in 1 MeV; the positron number density $dn/d\varepsilon$ is measured in 1 $\mathrm{cm}^{-3}\mathrm{MeV}^{1}$ in the comoving frame.

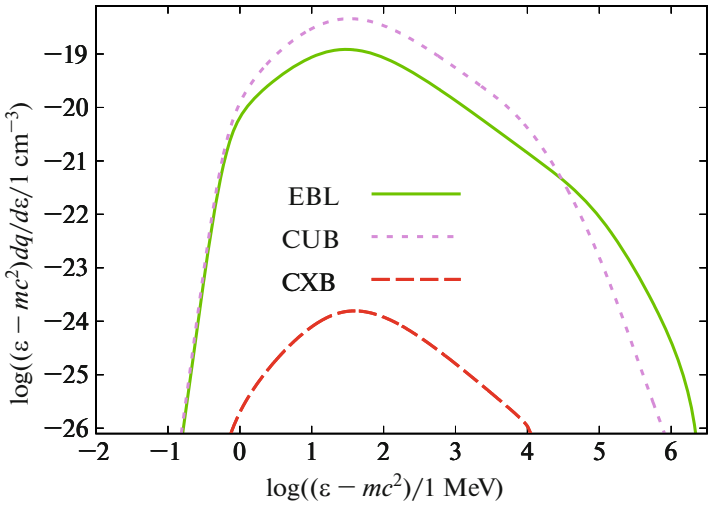


Fig. 4. Same as Fig. 3, but for $z = 1$.

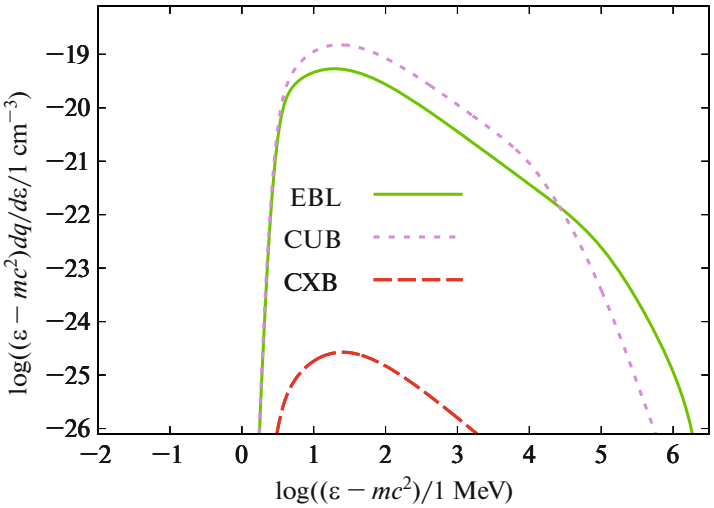


Fig. 5. Same as Fig. 3, but for $z = 2$.

number of positrons produced when CGB photons interact with hypothetical CUB photons may well be comparable to the contribution of the CGB+EBL process or even greater by several times. However, of course, in view of the intense absorption of ultraviolet photons in the interstellar gas, the real spectrum of CUB photons is most likely smaller by many orders of magnitude and their contribution to the total number of produced background positrons may be calmly neglected. At the same time, it should be noted that even with the addition of the upper limit of such positrons, their total number density is extremely low and does not exceed 10^{-18} cm^{-3} by $z = 0$. This is much lower than the number density of positrons that are produced by pulsars (Istomin et al. 2020). They give $\sim 3 \times 10^{34}$ s^{-1} per pulsar (Istomin et al. 2020) and, hence, one might expect that the number density of such positrons averaged over the volume of the Galaxy can reach $\lesssim 10^{-10}$ cm^{-3}, although actually it will be noticeably lower due to the annihilation of positrons in the Galactic disk. The number of positrons produced in the process under consideration will also be smaller than the number of positrons that are ejected by the jets of active galactic nuclei by many orders of magnitude (Nizamov and Pshirkov 2023, 2024). This number density can also be compared with the typical number density of positrons, $\sim 10^{-15}$–10^{-13} cm^{-3}, corresponding to the positron fluxes from Ma et al. (2023). It is also worth noting that microquasars and supernovae are believed to be the main sources of positrons in galaxies (Siegert et al. 2026). For example, it is thought that microquasars and supernovae in our Galaxy give more than 50 and 40% of the positrons, respectively; less than 10% of the positron production is left for the remaining sources, including the pulsars mentioned above (Siegert 2023). However, all these sources of positrons are localized in the vicinity of galaxies or in the vicinity of jet remnants, whereas the process under consideration creates a more or less homogeneous background of positrons spread over the entire Universe (see, however, Nizamov and Pshirkov 2024). The positrons produced when the hot-gas bremsstrahlung in galaxy clusters interact with CGB photons are more difficult to distinguish from the background positrons, since this leads to sources of positrons spread widely over the sky in view of the relatively large size of galaxy clusters.

FUNDING

This work was supported by ongoing institutional funding. No additional grants to carry out or direct this particular research were obtained.

CONFLICT OF INTEREST

The authors of this work declare that they have no conflicts of interest.

REFERENCES

1. M. Ackermann, M. Ajello, A. Albert, W. B. Atwood, L. Baldini, J. Ballet, G. Barbiellini, D. Bastieri, K. Bechtol, R. Bellazzini, E. Bissaldi, R. D. Blandford, E. D. Bloom, E. Bottacini, T. J. Brandt, J. Bregeon, P. Bruel, R. Buehler, S. Buson, G. A. Caliandro, R. A. Cameron, M. Caragiulo, P. A. Caraveo, et al., Astrophys. J. **799**, 86 (2015). https://doi.org/10.1088/0004-637x/799/1/86
2. P. A. R. Ade, N. Aghanim, M. Arnaud, M. Ashdown, J. Aumont, C. Baccigalupi, A. J. Banday, R. B. Barreiro, et al. (Planck Collaboration), Astron. Astrophys. **594**, 13 (2016). https://doi.org/10.1051/0004-6361/201525830
3. M. Ajello, J. Greiner, G. Sato, D. R. Willis, G. Kanbach, A. W. Strong, R. Diehl, G. Hasinger, N. Gehrels, C. B. Markwardt, and J. Tueller, Astrophys. J. **689**, 666 (2008). https://doi.org/10.1086/592595
4. P. S. Behroozi, R. H. Wechsler, and Ch. Conroy, Astrophys. J. **770**, 57 (2013). https://doi.org/10.1088/0004-637x/770/1/57
5. A. Cooray, R. Soc. Open Sci. **3**, 150555 (2013). https://doi.org/10.1098/rsos.150555
6. A. Franceschini, G. Rodighiero, and M. Vaccari, Astron. Astrophys. **487**, 837 (2008). https://doi.org/10.1051/0004-6361:200809691
7. S. A. Grebenev and R. A. Sunyaev, Astron. Lett. **45**, 791 (2020). https://doi.org/10.1134/s1063773719120016
8. R. J. Gould and G. P. Schréder, Phys. Rev. **155**, 1404 (1967). https://doi.org/10.1103/physrev.155.1404
9. R. Hill, K. W. Masui, and D. Scott, Appl. Spectrosc. **72**, 663 (2018). https://doi.org/10.1177/0003702818767133
10. Ya. N. Istomin, D. O. Chernyshov, and D. N. Sob'yanin, Mon. Not. R. Astron. Soc. **498**, 2089 (2020). https://doi.org/10.1093/mnras/staa2130
11. P.-X. Ma, Z.-H. Xu, Q. Yuan, X.-J. Bi, Y.-Z. Fan, I. V. Moskalenko, and Ch. Yue, Front. Phys. **18**, 44301 (2023). https://doi.org/10.1007/s11467-023-1257-7
12. B. A. Nizamov and M. S. Pshirkov, Astron. Lett. **49**, 9 (2023). https://doi.org/10.1134/s1063773723300011

13. B. A. Nizamov and M. S. Pshirkov, Astron. Lett. **50**, 186 (2024). https://doi.org/10.1134/s1063773724700087
14. A. N. Popov, D. P. Barsukov, A. V. Ivanchik, and S. V. Bobashev, Tech. Phys. **68**, 1619 (2023a).
15. A. N. Popov, D. P. Barsukov, A. V. Ivanchik, and S. V. Bobashev, Nauchno-Tekhnicheskie Vedomosti Sankt-Peterburgskogo Gosudarstvennogo Politekhnicheskogo Universiteta. Fiziko-Matematicheskie Nauki **16**, 429 (2023b). https://doi.org/10.18721/JPM.161.265
16. A. N. Popov, D. P. Barsukov, A. V. Ivanchik, and S. V. Bobashev, Tech. Phys. **70**, 2199 (2025).
17. T. Siegert, Astrophys. Space Sci. **368**, 27 (2023). https://doi.org/10.1007/s10509-023-04184-4
18. T. Siegert, F. Calore, P. Jean, M. Leising, N. De Séréville, G. H. Share, V. Tatischeff, W. Wang, and M.-R. Wu, Space Sci. Rev. **222**, 34 (2026). https://doi.org/10.1007/s11214-026-01281-y
19. A. Vikhlinin, A. Kravtsov, W. Forman, C. Jones, M. Markevitch, S. S. Murray, and L. Van Speybroeck, Astrophys. J. **640**, 691 (2006). https://doi.org/10.1086/500288

Translated by V. Astakhov

Publisher's Note. Pleiades Publishing remains neutral with regard to jurisdictional claims in published maps and institutional affiliations.

AI tools may have been used in the translation or editing of this article.